

Reconciling multi-messenger constraints with chiral symmetry restoration

Michał Marczenko,* Krzysztof Redlich, and Chihiro Sasaki

*Institute of Theoretical Physics, University of Wrocław,
plac Maksa Born 9, PL-50204 Wrocław, Poland*

(Dated: June 22, 2022)

We analyze the recent nuclear and astrophysical constraints in the context of a hadronic equation of state (EoS), in which the baryonic matter is subject to chiral symmetry restoration. We show that it is possible to reconcile the modern constraints on the neutron star (NS) radius and tidal deformability (TD) in the light of recent neutron skin thickness measurement by PREX-II experiment. We find that the softening of the EoS (required by the TD constraint) followed by a subsequent stiffening (required by the $2 M_\odot$ constraint) is driven by the appearance of Δ matter due to partial restoration of chiral symmetry. Sufficiently early onset of Δ matter lifts the tension between the results from the PREX-II experiment and TD from GW170817. We argue that a purely hadronic EoS that accounts for the fundamental properties of quantum chromodynamics (QCD) linked to the dynamical emergence of parity doubling with degenerate masses can be fully consistent with the nuclear and astrophysical constraints.

I. INTRODUCTION

The advancements of multi-messenger astronomy on different sources have led to remarkable improvements in constraining the equation of state (EoS) of dense, strongly interacting matter. The modern observatories for measuring masses and radii of compact objects, the gravitational wave interferometers of the LIGO-VIRGO Collaboration (LVC) [1, 2], and the X-ray observatory Neutron Star Interior Composition Explorer (NICER) provide new powerful constraints on their mass-radius (M-R) profile [3–6]. These stringent constraints allow for a detailed study of the neutron star (NS) properties and ultimately the microscopic properties of the EoS. In particular, the existence of $2 M_\odot$ NSs requires that the EoS must be stiff at intermediate to high densities to support them from gravitational collapse. At the same time, the tidal deformability (TD) constraint of a canonical $1.4 M_\odot$ NS from the GW170817 event implies that the EoS has to be fairly soft at intermediate densities. [7] suggested that the softening of the EoS at intermediate densities required to comply with the TD constraint, together with the subsequent stiffening at high densities required to support $2 M_\odot$ NSs, may be indicative for a phase transition in the stellar core. In several works, this transition was associated with a possible occurrence of a hadron-quark phase transition and, thus, the presence of deconfined quark matter. This has been achieved by systematic analyses of recent astrophysical observations within simplistic approaches, such as the constant-speed-of-sound (CSS) model [8–11]. Although such schemes are instructive, they are not microscopic approaches. They provide interesting heuristic guidance, but cannot replace more realistic dynamical models for the EoS, which accounts for the fundamental properties of quantum chromodynamics (QCD), the theory of strong interactions,

i.e., a self-consistent treatment of the chiral symmetry restoration in the baryonic sector. Recently, the possible phase transition to quark matter in the stellar core was also addressed in the supernova [12] and binary NS merger simulations [13, 14].

Recent neutron skin thickness analysis by the PREX-II experiment infers a large slope of the symmetry energy $L_{\text{sym}} = 106 \pm 37$ MeV at saturation [15]. Large upper bound for the parameter, $42 < L_{\text{sym}} < 117$ MeV, was also reported by the S π RIT Collaboration from the analysis of pion spectra produced in intermediate energy collisions [16]. Furthermore, the analysis of the PREX-II experiment within the energy density functionals (EFTs) yields $L_{\text{sym}} = 54 \pm 8$ MeV [17], which better agrees with the canonical estimates. Nevertheless, it is worthwhile to inspect the possible tension between the large value of L_{sym} and the NS properties inferred from multi-messenger measurements. It has been shown that the value of the parameter correlates with the TD of a $1.4 M_\odot$ NS under the assumption that the matter composition is purely nucleonic [15]. Consequently, large values of L_{sym} were excluded as they yield radii that do not meet the latest constraints from the GW170817 event [18, 19]. Moreover, such a large value of L_{sym} is at tension with astronomical observations [20]. Recently, this was also addressed in the context of first-order phase transition to quark matter within the CSS model [11, 21].

Understanding the NS physics is at the interface with QCD. Masses and radii of pulsars can provide stringent constraints on the EoS and phase structure of QCD in a region of the QCD phase diagram that is inaccessible to terrestrial experiments and present techniques of lattice QCD (LQCD) simulations. At the same time, the recent LQCD results exhibit a clear manifestation of the parity doubling structure for the low-lying baryons around the chiral crossover [22]. The masses of the positive-parity ground states are found to be rather temperature-independent, while the masses of negative-parity states drop substantially when approaching the chiral crossover temperature T_c . The parity doublet states become al-

* michal.marczenko@uwr.edu.pl

most degenerate with a finite mass in the vicinity of the chiral crossover. The observed behavior of parity partners is likely an imprint of the chiral symmetry restoration in the baryonic sector of QCD and is expected to occur also in cold dense matter. Such properties of the chiral partners can be described in the framework of the parity doublet model [23–25]. The model has been applied to hot and dense hadronic matter, neutron stars (see, e.g., [26–38]).

In this work, we utilize the parity doublet model for nucleonic and Δ matter [39] to investigate the implications on the structure of neutron stars in the light of the recent results from LIGO-VIRGO, NICER, and PREX-II experiments.

II. EQUATION OF STATE

A hadronic parity doublet model [39] is used to describe the NS properties. The model is composed of the baryonic parity doublets for the nucleon and $\Delta(1232)$ resonance, and mesons as in the Walecka model. In this work, we consider a system with $N_f = 2$. The baryonic degrees of freedom are coupled to the chiral fields (σ, π), the vector-isoscalar field (ω_μ), and the vector-isovector field (ρ_μ). The thermodynamic potential of the model in the mean-field approximation reads [39]

$$\Omega = V_\sigma + V_\omega + V_\rho + \sum_{x=N,\Delta} \Omega_x, \quad (1)$$

where the index x labels positive-parity and negative-parity spin-1/2 nucleons, i.e., $N \in \{p, n; p^*, n^*\}$, and spin-3/2 Δ 's, i.e., $\Delta \in \{\Delta_{++}, +, 0, -; \Delta_{++}^*, +, 0, -\}$. Note that the negative-parity states are marked with the asterisk. The mean-field potentials in Eq. (1) read

$$V_\sigma = -\frac{\lambda_2}{2}\sigma^2 + \frac{\lambda_4}{4}\sigma^4 - \frac{\lambda_6}{6}\sigma^6 - \epsilon\sigma, \quad (2a)$$

$$V_\omega = -\frac{m_\omega^2}{2}\omega^2, \quad (2b)$$

$$V_\rho = -\frac{m_\rho^2}{2}\rho^2, \quad (2c)$$

where $\lambda_2 = \lambda_4 f_\pi^2 - \lambda_6 f_\pi^4 - m_\pi^2$, and $\epsilon = m_\pi^2 f_\pi$. $m_\pi = 140$ MeV, $m_\omega = 783$ MeV, and $m_\rho = 775$ MeV are the π , ω , and ρ meson masses, respectively, and $f_\pi = 93$ MeV is the pion decay constant. The kinetic part of the thermodynamic potential, Ω_x , reads

$$\Omega_x = \gamma_x \int \frac{d^3p}{(2\pi)^3} T (\ln(1 - f_x) + \ln(1 - \bar{f}_x)), \quad (3)$$

where the factors $\gamma_N = 2$ and $\gamma_\Delta = 4$ denote the spin degeneracy of both parity partners for nucleons and Δ 's,

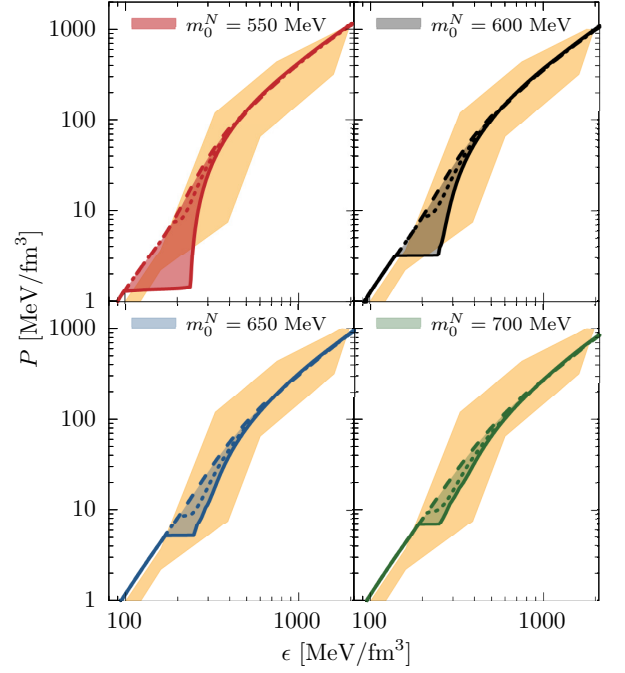


FIG. 1. Thermodynamic pressure, P , under the NS conditions of β -equilibrium and charge neutrality, as a function of the energy density, ϵ . The dashed lines correspond to the purely nucleonic EoSs. The solid lines correspond to the case $m_0^N = m_0^\Delta$. The region spanned between the two lines marks the results obtained for $m_0^N < m_0^\Delta$. The region enclosed by solid (dashed) and dotted lines show solutions where Δ matter enters the EoS through a first-order (crossover) transition. The orange-shaded region shows the constraint obtained by [40].

respectively. $f_x(\bar{f}_x)$ is the particle (antiparticle) Fermi-Dirac distribution function

$$f_x = \frac{1}{1 + e^{\beta(E_x - \mu_x)}}, \quad (4a)$$

$$\bar{f}_x = \frac{1}{1 + e^{\beta(E_x + \mu_x)}}, \quad (4b)$$

with β being the inverse temperature, the dispersion relation $E_x = \sqrt{\mathbf{p}^2 + m_x^2}$ and μ_x is the effective chemical potential.

The masses of the positive- and negative-parity chiral partners are given by

$$m_\pm^x = \frac{1}{2} \left[\sqrt{(g_1^x + g_2^x)^2 \sigma^2 + 4(m_0^x)^2} \mp (g_1^x - g_2^x) \sigma \right], \quad (5)$$

where \pm sign denotes parity and $x = N, \Delta$. The spontaneous chiral symmetry breaking yields the mass splitting between the two baryonic parity partners in each parity doublet. When the symmetry is restored, the masses in each parity doublet become degenerate: $m_\pm^x(\sigma = 0) = m_0^x$. The positive-parity nucleons are identified as the positively charged and neutral $N(938)$ states: proton (p) and neutron (n). Their negative-parity

counterparts, denoted as p^* and n^* , are identified as $N(1535)$ resonance [41]. The positive-parity Δ states are identified with $\Delta(1232)$ resonance. Their negative-parity chiral partners, Δ^* , are identified with $\Delta(1700)$ resonance [41]. For given chirally invariant mass, m_0^x , the parameters g_1^x and g_2^x are determined by the corresponding vacuum masses, $m_N = 939$ MeV, $m_{N^*} = 1500$ MeV, $m_\Delta = 1232$ MeV, $m_{\Delta^*} = 1700$ MeV.

The effective chemical potentials for nucleons and their chiral partners are given by

$$\mu_p = \mu_{p^*} = \mu_B + \mu_Q - g_\omega^N \omega - g_\rho^N \rho, \quad (6a)$$

$$\mu_n = \mu_{n^*} = \mu_B - g_\omega^N \omega + g_\rho^N \rho. \quad (6b)$$

The effective chemical potentials for Δ and their chiral partners are given by

$$\mu_{\Delta_{++}} = \mu_{\Delta_{++}^*} = \mu_B + 2\mu_Q - g_\omega^\Delta \omega - 3g_\rho^\Delta \rho, \quad (7a)$$

$$\mu_{\Delta_+} = \mu_{\Delta_+^*} = \mu_B + \mu_Q - g_\omega^\Delta \omega - g_\rho^\Delta \rho, \quad (7b)$$

$$\mu_{\Delta_0} = \mu_{\Delta_0^*} = \mu_B - g_\omega^\Delta \omega + g_\rho^\Delta \rho, \quad (7c)$$

$$\mu_{\Delta_-} = \mu_{\Delta_-^*} = \mu_B - \mu_Q - g_\omega^\Delta \omega + 3g_\rho^\Delta \rho. \quad (7d)$$

The constants, g_ω^x and g_ρ^x are the couplings of baryons to ω and ρ mesons, respectively [39].

The values of the λ_4 , λ_6 , and g_ω^N couplings are fixed by the properties of the nuclear ground state: the saturation density, $n_0 = 0.16 \text{ fm}^{-3}$, the binding energy, $\epsilon/n_B - m_N = -16$ MeV, and the compressibility, $K = 240$ MeV. The value of g_ρ^N can be fixed by fitting the value of symmetry energy, $E_{\text{sym}} = 31$ MeV. The couplings of the Δ resonance to the meson fields are poorly constrained due to limited knowledge from experimental observations. The most advocated constraint was obtained by the analysis of electromagnetic excitations of the Δ baryon within the framework of relativistic mean-field (RMF) model [42]. It puts a constraint on the relative strength of the scalar and vector couplings. Other phenomenological studies indicate an attractive $\Delta - N$ potential with no consensus on its actual size [43–46]. We note that in the parity doublet model the values of the nucleon- σ and $\Delta - \sigma$ couplings, g_1^x and g_2^x , are uniquely fixed by requiring the vacuum masses of the parity doublet states. On the other hand, the nature of the repulsive interaction among Δ resonances and their couplings to the ω and ρ mean fields are still far from consensus. For simplicity, in the present study, we fix their values $g_\omega^\Delta = g_\omega^N$ and $g_\rho^\Delta = g_\rho^N$. We note that, in general, additional repulsion between Δ 's would systematically shift their onset in the stellar sequence to higher densities. This eventually would prevent the neutron stars with Δ matter from existence in the gravitationally stable branch of the sequence. We note that this effect is similar as in the case of repulsive interactions between quarks [32].

In the present work, we take four representative values of $m_0^N = 550, 600, 650, 700$ MeV. Because the onset of Δ matter depends on the value of the chirally invariant mass m_0^Δ [39], we systematically study the influence of Δ on

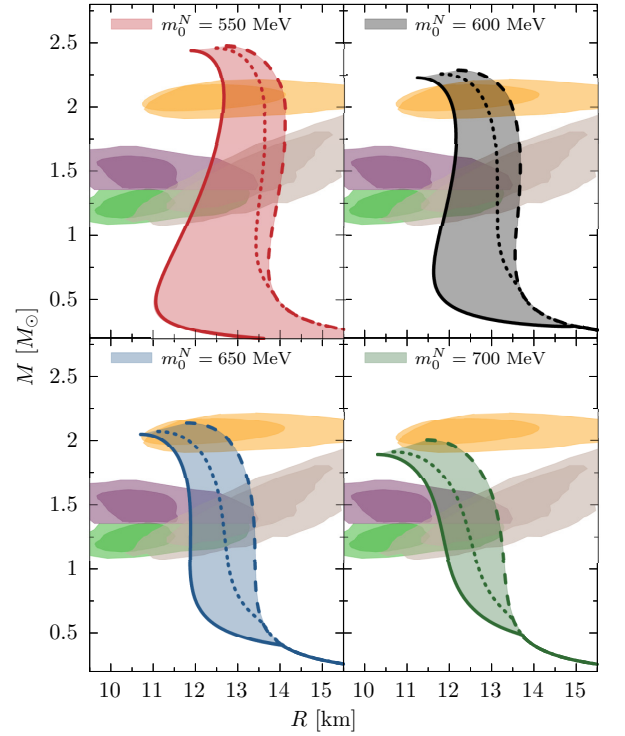


FIG. 2. Calculated M-R sequences. The meaning of the lines and color coding is the same as in Fig. 1. The inner (outer) orange bands show the 1σ credibility regions from the NICER analysis of observations of the massive pulsar PSR J0740+6620 as dark orange [4] and light orange [6]. The inner (outer) green and purple bands show 50% (90%) credibility regions obtained from the recent GW170817 [1] event for the low- and high-mass posteriors. The inner (outer) gray regions correspond to the M-R constraint at 68.2% (95.4%) obtained for PSR J0030+0451 by the group analyzing NICER X-ray data [6].

the EoS and compliance with astrophysical constraints, i.e., $M_{\text{max}} = (2.08 \pm 0.07) M_\odot$ [47] and $\Lambda_{1.4} = 190_{-120}^{+390}$ [1] constraints. In this work, we put an additional constraint on the chirally invariant mass of Δ . Namely, we require that $m_0^N \leq m_0^\Delta$. We chose this condition because too low values of m_0^Δ lead to the onset of Δ matter below the saturation density; thus, it spoils the properties of the ground state [39]. The difference between m_0^N and m_0^Δ can be attributed to the spin-spin interaction, similarly to hyper-fine splitting of the ground-state energy of the hydrogen atom in QED. We note that setting $m_0^\Delta = \infty$ suppresses the Δ states and the EoS effectively corresponds to the purely nucleonic EoS.

The predicted values of $L_{\text{sym}} \gtrsim 82$ MeV are larger than the recent chiral effective field theory [48] and density functional estimates [17]. On the other hand, they are fully consistent with the recent analysis of the neutron skin thickness by the PREX-II experiment, which inferred that $L_{\text{sym}} = 106 \pm 37$ MeV [15] and the range $42 < L_{\text{sym}} < 117$ MeV reported by the S π RIT Collaboration from the analysis of pion spectra produced in

m_0^N [MeV]	$R_{1.4}$ [km]	$\Lambda_{1.4}$	R_{max} [km]	M_{max} [M_\odot]
550	12.2, 14.0	506, 985	11.9, 12.7	2.44, 2.47
600	12.0, 13.7	394, 822	11.2, 12.2	2.23, 2.28
650	11.9, 13.4	321, 701	10.7, 11.8	2.05, 2.13
700	11.7, 13.1	275, 610	10.3, 11.5	1.89, 2.00

TABLE I. Properties of canonical $1.4 M_\odot$ and the maximum-mass NSs. Values for $m_0^\Delta = m_0^N$ and purely nucleonic EoSs are separated by comma.

intermediate energy collisions [16].

Fig. 1 shows the calculated EoSs under the NS conditions of β -equilibrium and charge neutrality for selected values of m_0^N . The orange-shaded area shows the constraint derived by requiring the maximum mass, obtained by [40] using a multi-polytrope ansatz for the EoS above the saturation density. To illustrate the effect of Δ matter on the EoS at intermediate densities, we show results obtained for purely nucleonic EoS (dashed line) together with the case $m_0^\Delta = m_0^N$ (solid line). The regions bounded by the two results correspond to the range spanned by solutions with $m_0^N < m_0^\Delta$ in each case. The region bounded by the solid and dotted lines corresponds to the range of EoSs with Δ appearing through a first-order transition. Consequently, the region between dotted and dashed lines shows the EoSs in which Δ matter appears smoothly. In general, the low-density behavior in each case is similar, until the deviations from the purely nucleonic EoSs are induced by the onset of Δ matter. The swift increase of the energy density is directly linked to the partial restoration of the chiral symmetry within the hadronic phase and resembled in the in-medium properties of dense matter in the parity doublet model. Most notably, it is associated with a drastic decrease of the negative-parity states in each parity doublet toward their asymptotic values, m_0^x . For instance, for $m_0^N = 550$ MeV, the EoSs with $m_0^\Delta \approx m_0^N$ result in an appearance of Δ matter through a strong first-order transition, which results in a large jump of the energy density. Consequently, the EoS underestimates the constraint at low densities. Interestingly, the softening is followed by a subsequent stiffening and the EoS reaches back the constraint at higher densities. This effect is more readily pronounced for smaller values of m_0^Δ . For other parametrizations shown in the figure, the EoSs fall into the region derived by the constraint.

III. PROPERTIES OF NEUTRON STARS

In Fig. 2, we show the M-R relations plotted up to the maximally stable solutions. Also shown are the state-of-the-art constraints: the high precision M-R analysis of the massive pulsar PSR J0740+6620 [4, 6] and PSR J0030+0451 [5] by the NICER collaboration, and the constraint from the recent GW170817 event [1]. The appearance of Δ matter affects the NS structure which is re-

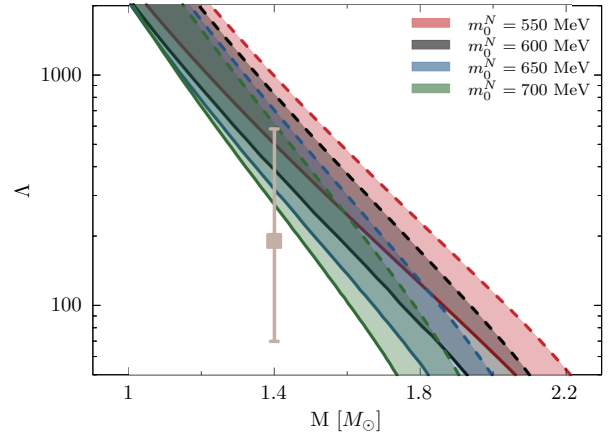


FIG. 3. TD parameter Λ as a function of neutron star mass. The error bar indicates the $\Lambda_{1.4} = 190^{+390}_{-120}$ constraint [2].

flected in the M-R relations. As discussed in the previous section, the softening of the EoS due to the appearance of Δ is followed by a subsequent stiffening of the EoS. As a consequence, a substantial reduction of the radii of a $1.4 M_\odot$ NSs is observed (see Table I). In particular, the radii of the $1.4 M_\odot$ NS obtained in the purely nucleonic EoS reduce from 14.4 km for $m_0^N = 700$ MeV, to almost 2 km for $m_0^N = 600$ MeV when $m_0^\Delta = m_0^N$ case is considered. On the other hand, the decrease of the star's maximum mass is seen only mildly (see Table I). This, in turn, is a consequence of the subsequent stiffening of the EoS at higher densities, which allows for the massive stars to sustain from the gravitational collapse. [49] have shown that the earlier onset of Δ matter yields a larger maximum mass. We note that this stays in contrast to our work, where we find a mild decrease of the maximum mass. This is due to additional softening of the EoS at high density that is provided by the onset of the negative-parity N^* and Δ^* . This highlights the importance of chiral symmetry restoration in dense matter on the properties of the NS structure.

In Fig. 3, we show the dimensionless TD parameter Λ as a function of the NS mass:

$$\Lambda = \frac{2}{3} k_2 C^{-5}, \quad (8)$$

where $C = M/R$ is the star compactness parameter. The parameter Λ can be computed through its relation to the Love number k_2 [50]. For the purely nucleonic case, higher values of m_0^N result in smaller values of TD. We note that even for $m_0^N = 700$ MeV, the purely nucleonic EoS is too stiff to comply with the constraint. Recently, [15] have shown that the stiffness of the EoS at intermediate densities is connected with its nuclear characteristics at saturation. Specifically, it is observed as a correlation between the value of TD of a $1.4 M_\odot$ NS and the value of L_{sym} at saturation. However, this conclusion is drawn upon the assumption that the EoS consists of

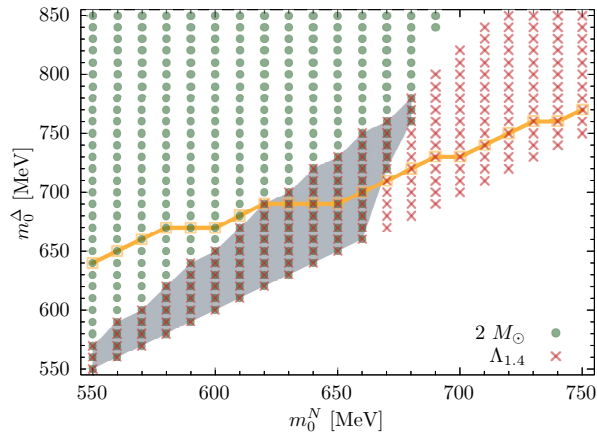


FIG. 4. Allowed combinations of the model parameters, m_0^N and m_0^Δ . The green circles indicate configurations that fulfill the lower bound for the maximum mass constraint, $M_{\text{max}} = (2.08 \pm 0.07) M_\odot$ [47]. The red crosses indicate configurations that are in accordance with the upper bound for the TD constraint, $\Lambda_{1.4} = 190^{+390}_{-120}$ [1]. The gray-shaded area shows the region where the two constraints are fulfilled simultaneously. The orange points show configurations with the largest value of m_0^Δ for which the Δ matter appears through the first-order transition.

purely nucleonic matter. Thus, the stiffness of the EoS due to large values of $L_{\text{sym}} \gtrsim 82$ MeV obtained in the parity doublet model creates tension with the TD constraint. The tension is commonly resolved with an onset of additional degrees of freedom at intermediate densities due to a strong first-order phase transition to quark matter [11, 21]. Such a conclusion about the existence of quark matter in the stellar core may, however, be premature. As we demonstrate in this work, strong phase transitions with a large latent heat may occur within hadronic matter due to the onset of Δ matter. This is seen in Fig. 3. If Δ matter is allowed in the EoS, TD reduces substantially, providing better agreement with the constraint. In general, smaller values of m_0^Δ , i.e., earlier onset of Δ matter, result in smaller TDs of a canonical $1.4 M_\odot$ NS. The most significant reduction of TD arises for $m_0^\Delta = m_0^N$ (see Table I). For a given value of m_0^N , the value of $\Lambda_{1.4}$ can be reduced significantly, while keeping the same value of the slope of the symmetry energy when Δ matter is considered. We note that the TD parameter requires sufficiently soft EoS at intermediate densities. This is seen in the figure, where the best agreement with the constraint is obtained for the smallest values of m_0^Δ . On the other hand, the $2 M_\odot$ requires a sufficiently stiff equation of state at higher densities. Inversely to TD, the most massive stars are obtained for the stiffest EoSs. Therefore, our results are following the TD and $2 M_\odot$ constraints, and the recent estimate of the parameter L_{sym} from the PREX-II experiment [15].

Lastly, we discuss the allowed parameter space. Fig. 4 shows the values of the chirally invariant masses, m_0^N and m_0^Δ for which the TD and $2 M_\odot$ constraints are met. The

TD constraint puts an upper limit on m_0^Δ and the purely nucleonic EoSs are ruled out. Therefore, the presence of Δ matter at intermediate densities is essential to comply with the TD constraint. The $2 M_\odot$ simultaneously constrains m_0^N from above and puts a lower limit on m_0^Δ . For sufficiently small m_0^Δ , the softening provided by the early onset of Δ matter is enough to satisfy both constraints. We conclude that the chirally invariant masses cannot be significantly different from each other and can be estimated to lie in the range from 550 to 680 MeV. The orange squares (connected with a line for readability) denote configurations with the largest value of m_0^Δ for which the Δ matter appears through a first-order transition. Configurations above the squares correspond to the onset via a smooth crossover transition.

Based on the above results, we conclude that the possibility of a smooth appearance of Δ matter is consistent with the astrophysical constraints and cannot be excluded at the moment. Nevertheless, the swift softening of the EoS at low densities is caused by the partial restoration of chiral symmetry whose remnants are expected to be apparent in the in-medium properties of cold baryonic matter even in the absence of a sharp first-order phase transition.

IV. CONCLUSION

In this work, we have shown that it is possible to reconcile the current constraints from terrestrial and multi-messenger measurements within a purely hadronic EoS, which accounts for the self-consistent treatment of the chiral symmetry restoration in the baryonic sector. To this end, we have adopted the parity doublet model for nucleonic matter including $\Delta(1232)$ resonance being subject to chiral symmetry restoration. We analyzed the properties of neutron stars in the light of the recent measurement of the neutron skin thickness by the PREX-II experiment [15] and S π RIT Collaboration [16]. We find that the scenario of the softening of the EoS at intermediate densities with the subsequent stiffening at high densities required by the $2 M_\odot$ and TD constraints can be realized within a hadronic EoS, where the softening of the EoS is obtained by an early onset of Δ matter due to partial restoration of chiral symmetry in the hadronic phase. Consequently, the radius of a canonical $1.4 M_\odot$ NS reduces substantially providing better agreement with the TD constraint from the GW170817 event, leaving the maximum mass in agreement with the $2 M_\odot$ constraint. In general, the softening of the EoS at intermediate densities due to the partial restoration of chiral symmetry allows for large values of L_{sym} at saturation. Thus, it lifts the tension between the nuclear characteristics at saturation and TD of a canonical $1.4 M_\odot$ NS. Moreover, as we have demonstrated in this work, it does not necessarily imply the existence of a hadron-quark phase transition as opposed to recent studies [11, 21].

ACKNOWLEDGEMENTS

This work was partly supported by the Polish National Science Center (NCN) under OPUS Grant No.

2018/31/B/ST2/01663 (K.R. and C.S.), and Preludium Grant No. UMO-2017/27/N/ST2/01973 (M.M.). K.R. also acknowledges the support of the Polish Ministry of Science and Higher Education. We acknowledge helpful comments from David Blaschke and Armen Sedrakian.

-
- [1] B. P. Abbott *et al.* (LIGO Scientific, Virgo), Phys. Rev. Lett. **121**, 161101 (2018), arXiv:1805.11581 [gr-qc].
 - [2] B. P. Abbott *et al.* (LIGO Scientific, Virgo), Phys. Rev. X **9**, 011001 (2019), arXiv:1805.11579 [gr-qc].
 - [3] T. E. Riley *et al.*, Astrophys. J. **887**, L21 (2019), arXiv:1912.05702 [astro-ph.HE].
 - [4] T. E. Riley *et al.*, Astrophys. J. Lett. **918**, L27 (2021), arXiv:2105.06980 [astro-ph.HE].
 - [5] M. C. Miller *et al.*, Astrophys. J. **887**, L24 (2019), arXiv:1912.05705 [astro-ph.HE].
 - [6] M. C. Miller *et al.*, Astrophys. J. Lett. **918**, L28 (2021), arXiv:2105.06979 [astro-ph.HE].
 - [7] F. J. Fattoyev, J. Piekarewicz, and C. J. Horowitz, Phys. Rev. Lett. **120**, 172702 (2018), arXiv:1711.06615 [nucl-th].
 - [8] M. G. Alford, S. Han, and M. Prakash, Phys. Rev. **D88**, 083013 (2013), arXiv:1302.4732 [astro-ph.SR].
 - [9] M. G. Alford and A. Sedrakian, Phys. Rev. Lett. **119**, 161104 (2017), arXiv:1706.01592 [astro-ph.HE].
 - [10] M. Cierniak and D. Blaschke, Astronomische Nachrichten **342**, 819 (2021).
 - [11] J. J. Li, A. Sedrakian, and M. Alford, (2021), arXiv:2108.13071 [astro-ph.HE].
 - [12] T. Fischer, N.-U. F. Bastian, M.-R. Wu, P. Baklanov, E. Sorokina, S. Blinnikov, S. Typel, T. Klähn, and D. B. Blaschke, Nat. Astron. **2**, 980 (2018), arXiv:1712.08788 [astro-ph.HE].
 - [13] A. Bauswein, N.-U. F. Bastian, D. B. Blaschke, K. Chatziioannou, J. A. Clark, T. Fischer, and M. Oertel, Phys. Rev. Lett. **122**, 061102 (2019), arXiv:1809.01116 [astro-ph.HE].
 - [14] E. R. Most, L. J. Papenfort, V. Dexheimer, M. Hanauske, S. Schramm, H. Stöcker, and L. Rezzolla, Phys. Rev. Lett. **122**, 061101 (2019), arXiv:1807.03684 [astro-ph.HE].
 - [15] B. T. Reed, F. J. Fattoyev, C. J. Horowitz, and J. Piekarewicz, Phys. Rev. Lett. **126**, 172503 (2021), arXiv:2101.03193 [nucl-th].
 - [16] J. Estee *et al.* (S π RIT), Phys. Rev. Lett. **126**, 162701 (2021), arXiv:2103.06861 [nucl-ex].
 - [17] P.-G. Reinhard, X. Roca-Maza, and W. Nazarewicz, (2021), arXiv:2105.15050 [nucl-th].
 - [18] A. Bauswein, O. Just, H.-T. Janka, and N. Stergioulas, Astrophys. J. Lett. **850**, L34 (2017), arXiv:1710.06843 [astro-ph.HE].
 - [19] E. Annala, T. Gorda, A. Kurkela, and A. Vuorinen, Phys. Rev. Lett. **120**, 172703 (2018), arXiv:1711.02644 [astro-ph.HE].
 - [20] C. Drischler, R. J. Furnstahl, J. A. Melendez, and D. R. Phillips, Phys. Rev. Lett. **125**, 202702 (2020), arXiv:2004.07232 [nucl-th].
 - [21] J.-E. Christian and J. Schaffner-Bielich, (2021), arXiv:2109.04191 [astro-ph.HE].
 - [22] G. Aarts, C. Allton, D. De Boni, and B. Jäger, Phys. Rev. **D99**, 074503 (2019), arXiv:1812.07393 [hep-lat].
 - [23] C. E. De Tar and T. Kunihiro, Phys. Rev. **D39**, 2805 (1989).
 - [24] D. Jido, T. Hatsuda, and T. Kunihiro, Phys. Rev. Lett. **84**, 3252 (2000), arXiv:hep-ph/9910375 [hep-ph].
 - [25] D. Jido, M. Oka, and A. Hosaka, Prog. Theor. Phys. **106**, 873 (2001), arXiv:hep-ph/0110005 [hep-ph].
 - [26] V. Dexheimer, S. Schramm, and D. Zschesche, Phys. Rev. **C77**, 025803 (2008), arXiv:0710.4192 [nucl-th].
 - [27] D. Zschesche, L. Tolos, J. Schaffner-Bielich, and R. D. Pisarski, Phys. Rev. **C75**, 055202 (2007), arXiv:nucl-th/0608044 [nucl-th].
 - [28] S. Benic, I. Mishustin, and C. Sasaki, Phys. Rev. **D91**, 125034 (2015), arXiv:1502.05969 [hep-ph].
 - [29] M. Marczenko and C. Sasaki, Phys. Rev. **D97**, 036011 (2018), arXiv:1711.05521 [hep-ph].
 - [30] M. Marczenko, D. Blaschke, K. Redlich, and C. Sasaki, Phys. Rev. **D98**, 103021 (2018), arXiv:1805.06886.
 - [31] M. Marczenko, D. Blaschke, K. Redlich, and C. Sasaki, Universe **5**, 180 (2019), arXiv:1905.04974 [nucl-th].
 - [32] M. Marczenko, D. Blaschke, K. Redlich, and C. Sasaki, Astron. Astrophys. **643**, A82 (2020), arXiv:2004.09566 [astro-ph.HE].
 - [33] M. Marczenko, K. Redlich, and C. Sasaki, Phys. Rev. D **103**, 054035 (2021), arXiv:2012.15535 [hep-ph].
 - [34] M. Marczenko, Eur. Phys. J. ST **229**, 3651 (2020), arXiv:2005.14535 [nucl-th].
 - [35] C. Sasaki and I. Mishustin, Phys. Rev. **C82**, 035204 (2010), arXiv:1005.4811 [hep-ph].
 - [36] T. Yamazaki and M. Harada, Phys. Rev. **C100**, 025205 (2019), arXiv:1901.02167 [nucl-th].
 - [37] Y. Motohiro, Y. Kim, and M. Harada, Phys. Rev. **C92**, 025201 (2015), [Erratum: Phys. Rev. **C95**, no. 5, 059903 (2017)], arXiv:1505.00988 [nucl-th].
 - [38] T. Minamikawa, T. Kojo, and M. Harada, Phys. Rev. C **103**, 045205 (2021), arXiv:2011.13684 [nucl-th].
 - [39] Y. Takeda, Y. Kim, and M. Harada, Phys. Rev. **C97**, 065202 (2018), arXiv:1704.04357 [nucl-th].
 - [40] K. Hebeler, J. M. Lattimer, C. J. Pethick, and A. Schwenk, Astrophys. J. **773**, 11 (2013), arXiv:1303.4662 [astro-ph.SR].
 - [41] P. A. Zyla *et al.* (Particle Data Group), PTEP **2020**, 083C01 (2020).
 - [42] K. Wehrberger, C. Bedau, and F. Beck, Nucl. Phys. A **504**, 797 (1989).
 - [43] Y. Horikawa, M. Thies, and F. Lenz, Nucl. Phys. A **345**, 386 (1980).
 - [44] J. S. O'Connell and R. M. Sealock, Phys. Rev. C **42**, 2290 (1990).
 - [45] J. Lehr, M. Effenberger, and U. Mosel, Nucl. Phys. A **671**, 503 (2000), arXiv:nucl-th/9907091.
 - [46] S. X. Nakamura, T. Sato, T. S. H. Lee, B. Szczerbinska, and K. Kubodera, Phys. Rev. C **81**, 035502 (2010),

- arXiv:0910.1057 [nucl-th].
- [47] E. Fonseca *et al.*, *Astrophys. J. Lett.* **915**, L12 (2021), arXiv:2104.00880 [astro-ph.HE].
- [48] T. Krüger, I. Tews, K. Hebeler, and A. Schwenk, *Phys. Rev. C* **88**, 025802 (2013), arXiv:1304.2212 [nucl-th].
- [49] J. J. Li, A. Sedrakian, and F. Weber, *Phys. Lett. B* **783**, 234 (2018), arXiv:1803.03661 [nucl-th].
- [50] T. Hinderer, *Astrophys. J.* **677**, 1216 (2008), arXiv:0711.2420 [astro-ph].